Sustainable Chemical Engineering
https://ojs.wiserpub.com/index.php/SCE/

UNIVERSAL WISER PUBLISHER

Research Article

Rapid Flash-Paper Combustion Synthesis of Technological Metals (Ag, Cu, Ni, Co)

Athanasios B. Bourlinos[1*], Dimitrios Moschovas[2], Apostolos Avgeropoulos[2], Theofanis N. Maimaris[2], Constantinos E. Salmas[2], Michael A. Karakassides[2]

[1]Physics Department, University of Ioannina, Ioannina, 45110, Greece
[2]Department of Materials Science & Engineering, University of Ioannina, Ioannina, 45110, Greece
E-mail: bourlino@uoi.gr

Received: 31 March 2026; **Revised:** 13 April 2026; **Accepted:** 20 April 2026

Abstract: A rapid, low-cost, and scalable flash-paper combustion method is presented for the synthesis of technologically important conductive (Ag, Cu) and magnetic (Ni, Co) metals. In this approach, nitrocellulose-based flash paper functions simultaneously as a fuel and an in situ reducing agent, enabling a self-sustained, highly exothermic reaction to take place. Metal salt-impregnated sheets, prepared from aqueous solutions, are simply dried and ignited, resulting in the rapid formation of metallic powders within seconds, without the need for external reducing agents or prolonged thermal processing. The resulting products were characterized using X-Ray Diffraction (XRD), confirming the formation of crystalline metallic phases, while electron microscopy revealed the formation of coarse, globular particles (30-90 μm) exhibiting compact morphology and low surface area (< 10 $m^2 \cdot g^{-1}$). Phase analysis further indicated high metal purity (> 90%) for Ag, Cu, and Ni, whereas Co exhibited comparatively lower purity due to its higher susceptibility to oxidation during combustion. Functional validation was achieved by demonstrating electrical conductivity (Ag, Cu) through simple paper-based circuits and magnetic behavior (Ni, Co) *via* magnetization measurements. In addition, the intense heat generated during combustion was explored for proof-of-concept thermal and thermophotovoltaic energy harvesting. Compared to conventional metallurgical and chemical reduction routes, this method offers a unique combination of operational simplicity, ultrafast processing, reduced energy input, and elimination of costly chemical reductants. These features position flash-paper combustion as a promising platform for scalable production of functional metals, particularly in decentralized or resource-limited settings.

***Keywords*:** flash-paper, nitrocellulose, conductive metals, magnetic metals, rapid combustion, scalable synthesis, heat harvesting

1. Introduction

Silver and copper, among the best electrical conductors, and nickel and cobalt, key magnetic materials, are widely used in electronics, energy systems, and advanced functional devices. Industrially, silver and copper are extracted by roasting their sulfide ores, whereas nickel and cobalt require roasting followed by carbothermal reduction.[1,2] Despite their industrial maturity, these conventional extraction and processing routes suffer from several critical limitations,

DOI: https://doi.org/10.37256/sce.7220269963

including high energy consumption, complex infrastructure requirements, and significant environmental impact. Consequently, there is a growing demand for alternative synthesis strategies that are rapid, energy-efficient, and adaptable to low-infrastructure environments.

To address this challenge, alternative approaches operating under significantly milder, and thus less energy-demanding conditions have been proposed, such as sodium borohydride reduction.[3,4] First developed during the Manhattan Project era, this method converts metal salts into their metallic form under mild conditions. However, the relatively high cost of $NaBH_4$ limits its applicability for large-scale metal extraction. In addition, $NaBH_4$ requires careful handling and controlled conditions, factors that further limit scalability and practical deployment. Therefore, there remains a clear need for simple, rapid, and cost-effective methods capable of producing functional metals without relying on expensive or hazardous reducing reagents.

In this context, cellulose derivatives provide attractive alternatives, offering abundant, low-cost, and environmentally benign reducing agents capable of operating under mild conditions. Recently, an innovative flash-paper combustion technique has been introduced as a powerful and straightforward method for synthesizing a wide range of materials.[5,6] It has been successfully applied to produce carbon, titanium dioxide (titania), cobalt blue ($CoAl_2O_4$), chromium(III) oxide green (Cr_2O_3), and various black magnetic spinel compounds (γ-Fe_2O_3, $CoFe_2O_4$, $NiFe_2O_4$). The core of this process relies on flash paper-essentially pure nitrocellulose-which combusts extremely rapidly and intensely, leaving virtually no solid ash or residue. Its naturally open, fibrous, and highly porous architecture enables exceptionally uniform uptake of precursor solutions: the sheet is soaked in an aqueous solution containing the desired precursor and allowed to dry. Igniting the dried, precursor-loaded flash paper initiates a rapid, self-propagating exothermic event that races through the sheet in mere seconds, requiring only a brief initial spark. This reaction fully converts the impregnated precursors into the target compound with remarkable operational simplicity, intense energy release, and very short processing times-features that make it promising for both exploratory materials synthesis and potential industrial scale-up under appropriate conditions.

While these studies demonstrated the versatility of flash-paper combustion for oxide and carbon materials, its applicability to the direct synthesis of elemental metals-particularly conductive and magnetic metals of technological importance-has not yet been systematically explored. This represents a critical research gap, as direct metal formation typically requires controlled reducing environments or external reducing agents. Importantly, the combination of rapid heat release and the intrinsic reducing capability of the decomposing cellulosic matrix create a unique reaction environment that can potentially enable in situ reduction of metal salts to their metallic state. This combined capability distinguishes flash-paper combustion from conventional combustion synthesis and solution-based reduction techniques.

In this work, the scope of flash-paper combustion is extended to the direct synthesis of technologically relevant metals-silver (Ag), copper (Cu), nickel (Ni), and cobalt (Co)-from their respective salt precursors. The novelty of this study lies in (i) the demonstration of a single-step, ultrafast route for producing both conductive and magnetic metals, (ii) the elimination of external chemical reducing agents, and (iii) the simultaneous exploration of heat generation for potential energy harvesting applications. Specifically, flash paper is soaked in aqueous solutions of silver nitrate, copper nitrate, nickel acetate, or cobalt acetate, dried, and then ignited to produce the target metals as micron-sized powders *via* a rapid exothermic process. The heat released during this self-sustained combustion facilitates the in situ reduction of the metal salts and simultaneously presents an opportunity for thermal energy harvesting (e.g., boiling a working fluid or thermophotovoltaic conversion, as demonstrated in this work). The conductive nature of Ag and Cu is demonstrated *via* simple paper circuits using a conductive paste prepared with water glass (sodium silicate solution), while the magnetic behavior of Ni and Co is confirmed by their attraction to a strong permanent magnet and by magnetization measurements.

Overall, the primary objective of this study is to develop and validate a rapid, energy-efficient flash-paper combustion method for the direct synthesis of conductive (Ag, Cu) and magnetic (Ni, Co) metals. Secondary objectives include (i) characterizing the structural and morphological properties of the synthesized metals, (ii) demonstrating their functional electrical and magnetic performance, and (iii) evaluating the potential of the process for heat and energy harvesting applications.

2. Materials and methods

2.1 *Flash-paper combustion synthesis of metals*

Flash paper, commonly used in magic performances to create visual effects, is a flammable material that burns quickly with a bright flash. When used in small quantities, it can be handled safely at the laboratory scale.

Rectangular pieces of thick flash paper (6.5 × 12.5 cm, thickness 0.3 mm, average mass 0.45 ± 0.05 g per piece, MagicStar) were impregnated with aqueous metal salt solutions prepared using deionized water. After draining, the samples were dried at 90 °C for 45 min in a convection oven under ambient atmosphere (relative humidity 40-50%) and subsequently ignited in a porcelain crucible. Ignition was performed using butane lighter under ambient air conditions (20 °C), and the combustion duration was < 5 s. This triggered a rapid, self-sustained combustion process (350-450 °C),[5] yielding metallic products within seconds. The resulting powders were collected after natural cooling to room temperature (5 min). All products exhibited low Brunauer-Emmett-Teller (BET) N_2 surface areas (< 10 $m^2 \cdot g^{-1}$).

Key input parameters controlling the synthesis included: (i) precursor concentration (20-40%), (ii) impregnation time (1 min), (iii) drying temperature and duration, and (iv) ambient atmospheric conditions. These parameters were kept constant across all experiments to ensure comparability of results.

For silver, flash paper pieces were immersed in a 20% $AgNO_3$ solution (Alfa Aesar, 99.9995%), producing approximately 10 ± 1 mg of metallic silver per piece. The resulting product was washed with 1 M $NH_3 \cdot H_2O$ for 15 min at room temperature (20 °C) to remove residual silver oxide. Copper was prepared analogously using a 40% $Cu(NO_3)_2 \cdot 3H_2O$ solution (Fluka, > 98%), yielding 10 ± 1 mg of metallic copper per piece; the product was subsequently treated with 1 M HCl for several hours at room temperature to restore its characteristic luster.

Nickel was obtained from an approximately 20% $Ni(CH_3COO)_2 \cdot 4H_2O$ solution (Aldrich, 98%), yielding 5.0 ± 0.5 mg per piece, and was purified by treatment with 10% acetic acid at 90 °C for 1 h to remove residual nickel oxide to the greatest extent possible. Cobalt was synthesized following the same procedure using an approximately 20% $Co(CH_3COO)_2 \cdot 4H_2O$ solution (Acros Organics, 97%), producing 7.0 ± 0.5 mg per piece, with post-treatment in 1% acetic acid for 1 h at room temperature to minimize cobalt oxide impurities.

The overall yield reproducibility across samples was within ± 10%, demonstrating acceptable experimental consistency.

2.2 *Characterization techniques*

X-Ray Diffraction (XRD) measurements in powder form were carried out on a Bruker D8 Advance diffractometer (Bruker AXS GmbH, Karlsruhe, Germany) with Cu Kα radiation (λ = 1.54 Å), using a glass holder. Data were collected in the 2θ range of 20-80° with a step size of 0.02° and a scan rate of 1° min^{-1}. Phase identification was performed using standard ICDD PDF-2 database references. Scanning Electron Microscopy (SEM) images were obtained using a JEOL JSM-6510LV SEM Microscope (JEOL Ltd., Tokyo, Japan) equipped with an X-Act Energy Dispersive X-ray Spectroscopy (EDS) detector by Oxford Instruments (Abingdon, Oxfordshire, UK) for energy dispersive X-ray spectroscopy, with an acceleration voltage of 20 kV applied. Particle size distributions were estimated from SEM images by analyzing at least 50 particles using image analysis software, yielding average particle sizes in the micrometer range. Elemental composition and purity of the samples were confirmed by EDS analysis, showing dominant signals corresponding to the respective metals (Ag, Cu, Ni, Co) with moderate oxygen contributions attributed to surface oxidation. Nitrogen (N_2) adsorption-desorption isotherms were measured by an ASAP 2460 analyzer (Micromeritics, Norcross, GA, USA) by using ultrahigh pure N_2 (99.999%). The samples were outgassed for 10 h under vacuum (10^{-4} mbar) at 120 °C. Porosimetry isotherms were recorded at 77 K using a liquid N_2 Dewar vessel at relative pressures (P/P_o) ranging from 10^{-2} to 0.99, and the specific surface areas were calculated using the BET method. Electrical conductivity of Ag and Cu powders was qualitatively evaluated by incorporating the powders into a sodium silicate binder to form conductive pastes, followed by two-point probe measurements on paper substrates. Magnetic measurements in powdered form (e.g., magnetization *vs.* applied magnetic field) were carried out at room temperature using a Lakeshore 7300 Vibrating Sample Magnetometer (VSM) (Lake Shore Cryotronics, Inc., Westerville, OH, USA). Hysteresis loops were recorded in the field range of -20 to + 20 kOe, enabling determination of saturation magnetization, coercivity, and remanence.

3. Results and discussion

3.1 *Conductive metals*

Figure 1 illustrates the flash-paper combustion synthesis process, in which nitrocellulose acts as both a fuel and a reducing agent, promoting the decomposition of metal nitrates and the formation of metallic silver (top row) and copper (bottom row). The left and middle columns of the figure show sequential stages of the combustion: shortly after ignition, intense flames envelop the impregnated flash paper in a ceramic dish, accompanied by visible gas evolution and rapid consumption of the nitrocellulose substrate. The combustion is vigorous and completes within seconds, leaving behind the metallic product. The right column displays the final as-synthesized powders collected in glass vials: dark gray Ag powder (top) and reddish-brown Cu powder (bottom), consistent with the characteristic appearances of elemental silver and copper, respectively.

Figure 1. Flash-paper combustion synthesis of silver (top row) and copper (bottom row). From left to right, each sequence shows ignition of flash paper impregnated with silver nitrate or copper nitrate, respectively. Ignition initiates a self-sustaining exothermic reaction, driving rapid decomposition of the metal nitrate and resulting in the formation of elemental silver or copper. The vials on the right show the collected metallic products after completion of the reaction

The overall process proceeds *via* redox reactions in which nitrocellulose, approximated by the average empirical formula $C_6H_{7.6}O_{8.4}N_{2.4}$,[7] acts as a reducing agent for the metal nitrates, converting the metal ions to their zero-valent states while itself oxidizing to gaseous products, primarily N_2, CO_2, and H_2O. The reactions can be represented by the following balanced equations:

$$74\ AgNO_3 + 30\ C_6H_{7.6}O_{8.4}N_{2.4} \rightarrow 74\ Ag + 73\ N_2 + 180\ CO_2 + 114\ H_2O \quad (1)$$

$$37\ Cu(NO_3)_2 + 30\ C_6H_{7.6}O_{8.4}N_{2.4} \rightarrow 37\ Cu + 73\ N_2 + 180\ CO_2 + 114\ H_2O \quad (2)$$

In these schemes, the reduction of Ag^+ and Cu^{2+} ions is driven by the intrinsically reducing nature of the cellulosic matrix, which contains a high density of hydroxyl functionalities.[8,9] Together with the extremely high local temperatures generated during nitrocellulose combustion, this environment further promotes rapid decomposition of the nitrate precursors and facilitates reduction of the metal ions to their metallic states.

Figure 2 displays the XRD patterns of the synthesized silver and copper samples, along with their corresponding reference patterns from the International Centre for Diffraction Data (ICDD) PDF-2 (2022) database. The XRD pattern

of the Ag sample exhibits characteristic sharp diffraction peaks at approximately 2θ = 38.1°, 44.3°, 64.4°, and 77.5°, which are indexed to the (111), (200), (220), and (311) planes of metallic silver,[10] in excellent agreement with the standard reference PDF #01-071-3762. Similarly, the Cu sample shows well-defined sharp peaks at approximately 2θ = 43.3°, 50.4°, and 74.1°, corresponding to the (111), (200), and (220) planes of metallic copper[11] (PDF #01-070-3039). The diffraction peaks are broader in the silver compared to the copper sample throughout the measured 2θ range, indicating a smaller average crystallite size in the former case (see below). Notably, no additional peaks attributable to oxide phases are observed in either pattern, confirming the high phase purity of both metallic products. Silver and copper exhibit relatively low tendencies toward oxidation due to their positive standard reduction potentials (+ 0.80 V for Ag and + 0.34 V for Cu), rendering oxidation thermodynamically less favorable compared to more reactive metals.

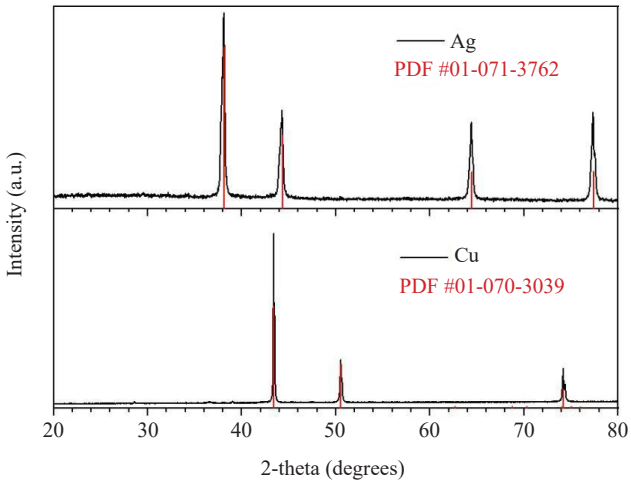

Figure 2. XRD patterns of the derived silver (top) and copper (bottom) along with the corresponding ICDD PDF cards for Ag (PDF #01-071-3762) and Cu (PDF #01-070-3039)

Crystallite size estimation from XRD data is commonly based on Scherrer equation, which, however, is primarily applicable to nanoscale materials with significant peak broadening. For bulk particles with sharp reflections, as in the present work, peak broadening is minimal and often dominated by instrumental effects and lattice strain, making size estimates unreliable. In such cases, electron microscopy techniques are preferred, as they allow direct visualization and measurement of particle size.

Accordingly, the SEM images in the top row of Figure 3 reveal predominantly globular silver particles (*ca.* 30 μm) with a uniform surface elemental distribution (98% Ag). By comparison, the bottom row shows larger globular copper particles (*ca.* 90 μm) with chemical mapping also indicating a dense and homogeneous distribution (97% Cu). These results highlight clear differences in particle size between the silver and copper samples, consistent with the XRD data. In both samples, much smaller particles were also observed, though in considerably lower abundance. Owing to their micron-scale dimensions, both samples exhibit very low specific surface areas (< 10 $m^2 \cdot g^{-1}$), in agreement with the inverse scaling of BET surface area with particle diameter ($S \propto 1/d$),[12] whereby compact, non-porous micron-sized particles inherently display extremely low values.[13] These observations can be further contextualized by comparison with literature reports employing sodium borohydride reduction,[3] where nanoscale particles with higher surface areas are typically obtained. In contrast, the present approach yields micron-sized, compact particles, highlighting a clear distinction in morphology and scale relative to nanoparticle-forming synthesis routes.[4]

The formation of micrometer-scale metal particles in flash paper combustion synthesis can be attributed to the extreme transient temperatures generated during nitrocellulose ignition, which promote rapid sintering and coalescence of initially formed nuclei. Simultaneously, the vigorous evolution of gaseous products induces particle collisions and aggregation within the combustion zone, further enhancing growth into larger structures. Additionally, although the process is rapid, the cooling rate is possibly insufficient to quench and stabilize nanoscale features, allowing continued

diffusion-driven growth and consolidation before solidification, ultimately resulting in bulk-like particles on the order of tens of micrometers.[14,15]

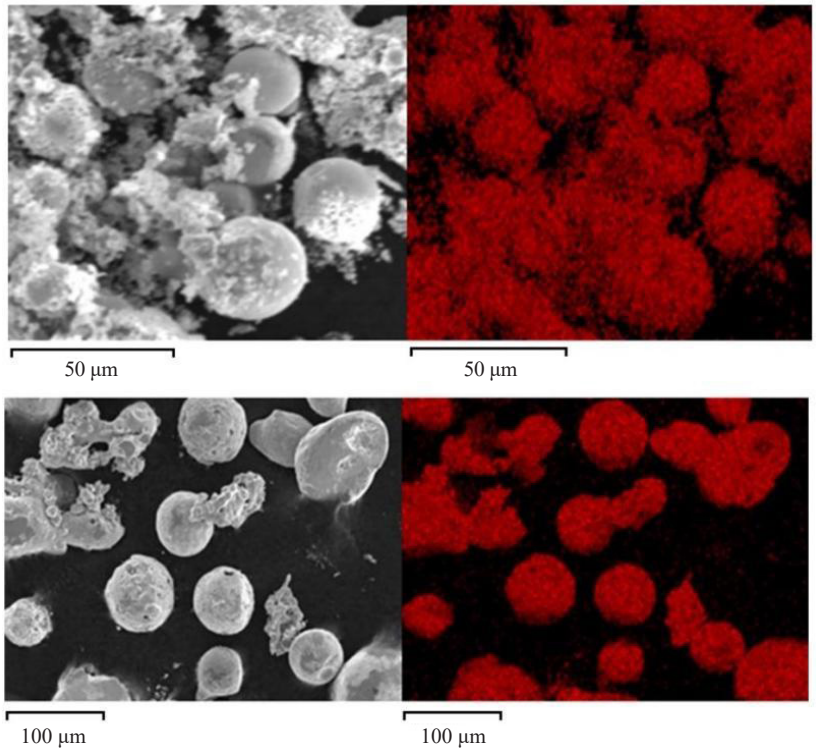

Figure 3. Top: SEM image and Ag elemental map (red) of the silver sample (scale bar 50 µm). Bottom: SEM image and Cu elemental map (red) of the copper sample (scale bar 100 µm)

In order to demonstrate the conductive nature of the metals, silver was formulated into a conductive paste (70% Ag, within the typical 65-80% range of many commercial silver pastes) using water glass (sodium silicate solution, Merck) as a binder. Sodium silicate is a charged, linear inorganic polymer that adsorbs onto particle surfaces, stabilizing the suspension through electrostatic repulsion. The paste was applied onto paper with a small brush to create two parallel conductive traces, forming a simple yet flexible circuit pathway after drying. A Light Emitting Diode (LED) was fixed at one end of the traces using tape to ensure good electrical contact, while a 9 V battery was connected to the opposite end using clips. Upon completing the circuit, the LEDs (red and blue) illuminated successfully, clearly demonstrating the effective electrical conductivity of the as-synthesized silver and its potential use in low-cost paper-based electronic devices[16,17] (Figure 4).

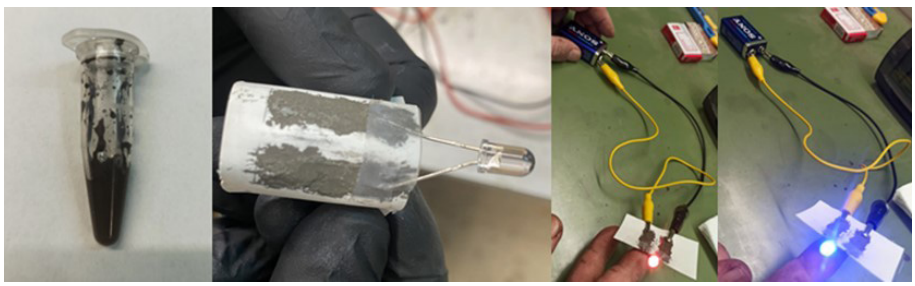

Figure 4. From left to right: conductive silver paste prepared from derived silver metal and water glass (70% Ag); application of the paste onto paper using a small brush to form two parallel conductive traces, along with attachment of an LED at one end of the traces using tape; connection of a 9 V battery at the opposite end *via* clips, resulting in illumination of red or blue LEDs

Silver proved to be particularly suitable for this application due to its smaller particle size, which enabled uniform dispersion in the binder and the formation of continuous conductive pathways after drying. In contrast, although copper exhibited good intrinsic conductivity when tested using a two-point multimeter, its incorporation into the paste was challenging because of the larger grain size of its particles. This led to phase separation within the mixture and, after drying, poor conductivity resulting from large voids between particles that hindered effective electrical contact.

3.2 *Magnetic metals*

Magnetic nickel and cobalt were similarly produced *via* flash-paper combustion using nickel acetate and cobalt acetate precursors (Figure 5). Nitrocellulose sheets impregnated with the respective acetate solutions were ignited, triggering a rapid, self-sustaining exothermic reaction that consumed the substrate within seconds and yielded Ni or Co as the solid residue.

Figure 5. Rapid flash-paper combustion synthesis of nickel (top row) and cobalt (bottom row). From left to right, each sequence depicts the ignition of flash paper impregnated with either nickel acetate or cobalt acetate, leading to a bright, self-sustained combustion reaction. The images on the right display the resulting magnetic metals collected inside vials, visibly attracted to the side by a strong external magnet

The transformation is governed by redox processes involving both the nitrocellulose matrix and the acetate ligands. During combustion, nitrocellulose decomposes to generate heat and reactive gaseous species, while the acetate groups provide additional reducing equivalents through oxidative decomposition to CO_2 and H_2O. Collectively, these processes convert Ni^{2+} and Co^{2+} ions to their zero-valent metallic forms, as summarized by the following reactions:

$$5\ Ni(CH_3COO)_2 + 5\ C_6H_{7.6}O_{8.4}N_{2.4} + 36\ O_2 \rightarrow 5\ Ni + 6\ N_2 + 50\ CO_2 + 34\ H_2O \quad (3)$$

$$5\ Co(CH_3COO)_2 + 5\ C_6H_{7.6}O_{8.4}N_{2.4} + 36\ O_2 \rightarrow 5\ Co + 6\ N_2 + 50\ CO_2 + 34\ H_2O \quad (4)$$

In this mechanism, the combined reducing action of the hydroxyl groups of the cellulosic backbone[18,19] and the carboxylate groups of the acetate moieties[20,21] create a strongly reducing environment that, together with the heat generated during combustion, enables efficient conversion of Ni^{2+} and Co^{2+} to metallic nickel and cobalt.

The XRD patterns of the synthesized Ni and Co samples are presented in Figure 6. For the Ni sample, sharp diffraction peaks are observed at 2θ values around 44.5°, 51.8°, and 76.3°, which correspond to the (111), (200), and

(220) planes of metallic Ni (PDF #01-071-3740).[22] Minor reflections attributed to NiO (PDF #01-071-4751)[23] are also observed, indicating the presence of a small fraction of NiO, likely formed through partial oxidation during synthesis. Rietveld refinement analysis quantifies the phase composition as approximately 92% metallic Ni and 8% NiO. For the Co sample, the sharp diffraction peaks at approximately 44.2°, 51.5°, and 75.9° correspond to the (111), (200), and (220) planes of metallic Co (PDF #00-015-0806).[24] Additional peaks assigned to CoO (PDF #01-070-2857)[25] confirm partial oxidation of cobalt. Rietveld refinement reveals a higher degree of oxidation compared to the Ni sample, with the sample consisting of approximately 63% metallic Co and 37% CoO. Both nickel and cobalt are susceptible to oxidation due to their negative standard reduction potentials (-0.25 V for nickel and -0.28 V for cobalt). The slightly more negative reduction potential of cobalt, combined with differences in oxide stability, surface reactivity, and oxidation kinetics, contribute to the greater extent of oxidation observed in the Co sample. Such partial oxidation is commonly observed in combustion-based syntheses, where the rapid reaction occurs in ambient atmosphere and freshly formed metal particles can undergo surface oxidation during cooling and exposure to air.

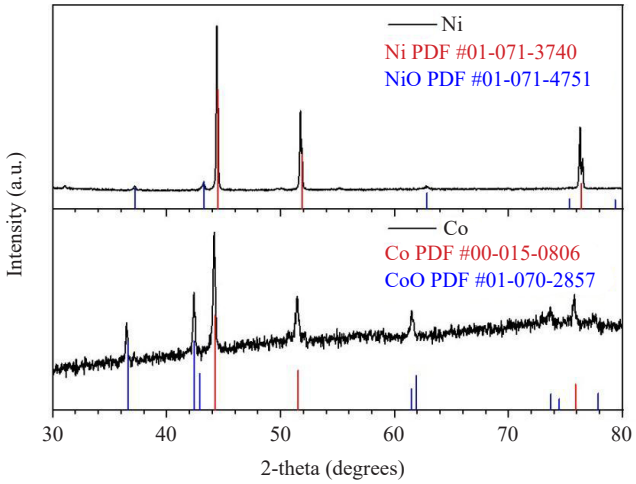

Figure 6. XRD patterns of Ni and Co samples. The reference lines indicate metallic and oxide phases: red lines correspond to the metallic phases-Ni (PDF #01-071-3740) and Co (PDF #00-015-0806)-and blue lines correspond to the oxide phases-NiO (PDF #01-071-4751) and CoO (PDF #01-070-2857)

The SEM images in Figure 7 show Ni (top row) and Co (bottom row) as compact, globular particles (*ca.* 70 μm and *ca.* 50 μm, respectively) with uniform surface elemental distributions (92% Ni and 96% Co, respectively). As with the silver and copper samples, smaller particles were also present to a much lesser extent. The predominantly coarse morphology is consistent with the high-temperature, gas-evolving combustion environment, which promotes particle coalescence and limits effective quenching of finer features.[14,15] Consequently, the relatively large particle sizes result in very low specific surface areas (< 10 $m^2 \cdot g^{-1}$).[13] Once again, in contrast to sodium borohydride reduction methods that typically yield nanoscale particles,[3,4] the present approach produces micron-sized, compact structures, underscoring a distinct morphological regime.

The magnetization behavior of the samples was analyzed quantitatively at room temperature, as illustrated by the isothermal hysteresis loops shown in Figure 8. The saturation magnetization values are 44.8 emu·g^{-1} for Ni and 89.5 emu·g^{-1} for Co, corresponding to 81% and 55% of the respective bulk values (55 emu·g^{-1} for Ni and 162 emu·g^{-1} for Co).[26] These bulk values are characteristic of materials with dimensions exceeding the nanoscale threshold (> 0.1 μm), which is consistent with the micron-sized particles observed in the present study. Therefore, the reduced magnetization of the powders relative to the bulk materials can be primarily attributed to oxide formation during synthesis, as supported by the XRD results, rather than to particle size effects. Notably, the 81% and 55% magnetization values for Ni and Co fairly match the phase purities of 92% and 63%, respectively, as determined by Rietveld analysis. Lastly, both samples exhibit soft ferromagnetic behavior with relatively low coercive field (25-35 Oe) and reduced remanent magnetization (1.3-2.3 emu·g^{-1}), consistent with values reported for bulk nickel and cobalt.[27,28] These properties make the Ni and Co

powders suitable for applications in magnetic separation systems and soft magnetic components.

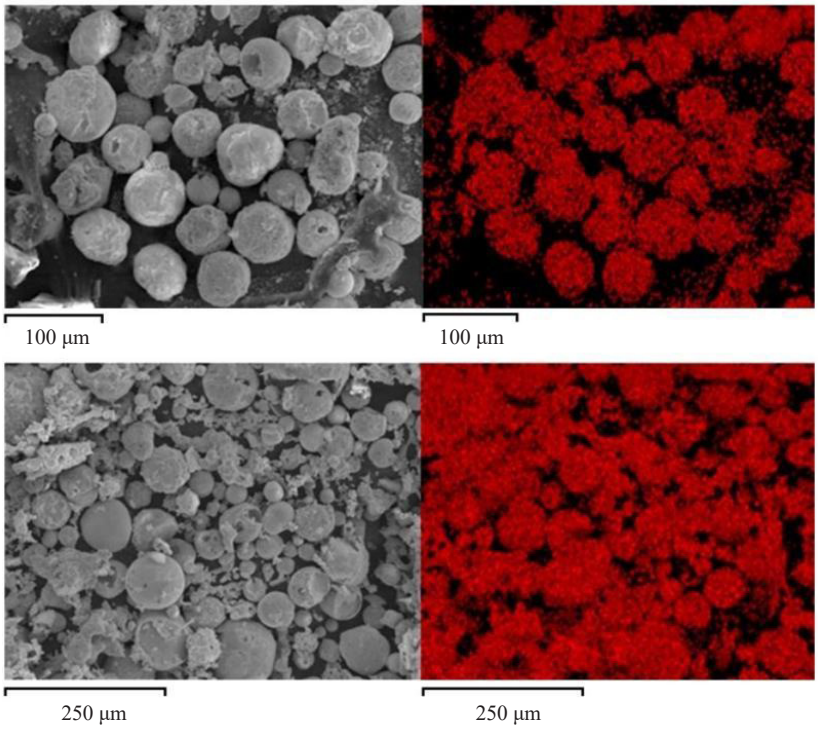

Figure 7. Top: SEM image and Ni elemental map (red) of the nickel sample (scale bar 100 µm). Bottom: SEM image and Co elemental map (red) of the cobalt sample (scale bar 250 µm)

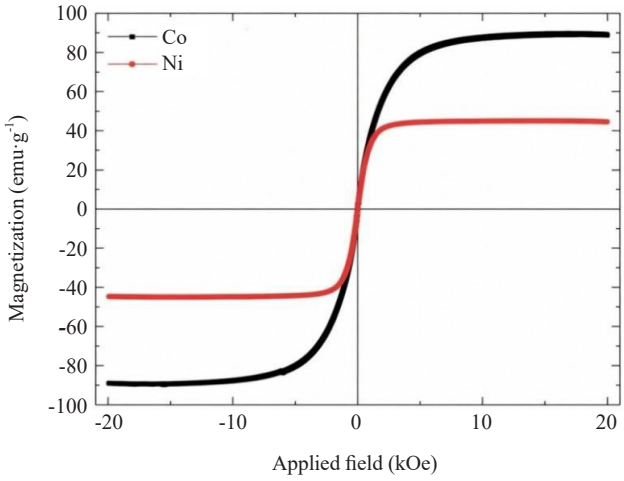

Figure 8. Magnetization *vs.* applied magnetic field hysteresis loops of Co and Ni samples measured at room temperature

3.3 *Potential for scale up and heat harvesting*

Although the present experiments were conducted at laboratory scale, the concept suggests a possible pathway toward continuous processing configurations that could combine precursor impregnation, rapid energetic conversion, and heat recovery. Flash combustion of impregnated nitrocellulose substrates liberates substantial thermal energy in

a self-sustaining manner while simultaneously reducing precursor metal compounds to recoverable metallic forms. Translation of this approach to an industrial scale would require a continuous and integrated processing scheme coupling wet impregnation, drying, controlled energetic reaction, product collection, and heat scavenging.

In such an envisioned system, rolls of nitrocellulose paper would pass continuously through a bath containing a metal-bearing solution, soaking up the precursors like a sponge. The saturated sheets would then enter a multi-stage drying oven designed to remove residual solvent uniformly, minimizing heterogeneity that could otherwise lead to uneven reaction propagation. After drying, automated cutting would divide the substrate into precisely defined portions before introduction into a combustion chamber. There, sequenced ignition pulses would trigger rapid, spatially confined energy releases in controlled succession rather than a single large-scale event. The released thermal energy could be harvested through multiple pathways. One primary route involves transferring heat to a water-jacketed heat exchanger, where the heat vaporizes a working fluid-for instance, as an illustrative analogue, low-boiling acetone[29] (boiling point ≈ 56 °C) (Figure 9)-producing pressurized vapor that could expand in a turbine to generate electricity.

Figure 9. Low-boiling acetone brought to reflux (middle & right photos) by heat released from the combustion of cobalt acetate-impregnated flash paper, serving as a small-scale analogue for steam generation in turbine-driven electrical systems. The photo on the left shows acetone solvent at room temperature prior to igniting the impregnated flash paper

Alternatively, a thermophotovoltaic setup[30] could convert that radiant heat directly into electrical current-similar to how a small-scale system might use the glow from a hot emitter to illuminate an LED *via* photovoltaic cells tuned to infrared wavelengths (Figure 10). In parallel with both types of energy harvesting, the reaction products would be collected as particulate solids, which would likely require downstream consolidation, purification, or refinement before any practical metallurgical use. In the present case, the powders have particle sizes in the tens of micrometers range, which significantly reduces the likelihood of airborne dispersion compared to nanoscale materials. Furthermore, the magnetic nature of Ni and Co promotes aggregation and densification, further limiting the potential for particle release. Therefore, concerns related to exhaust or particle emission are not applicable under the conditions considered in this work.

Chaining impregnation, energetic reaction control, metal recovery, and heat harvesting into a single continuous operation presents a theoretically elegant integration of materials processing and energy release. In practice, however, any such scheme would be constrained by extensive safety engineering, regulatory compliance, and risk-mitigation requirements associated with handling nitrated polymers in continuous industrial environments. Moreover, nitrocellulose itself represents a fundamental economic limitation, owing to its limited availability and nontrivial production cost. Taken together, these factors imply that, even with optimized engineering, this flash-paper-inspired approach may not currently outcompete established metallurgical routes for bulk industrial production. Further work is required to enhance metal yield and minimize the formation of undesired oxide phases by optimizing the amount of starting materials and more precisely controlling the reaction atmosphere, for example through the use of inert gas environments (e.g., Ar or N_2), to suppress oxidation during the combustion process.

Figure 10. Alternative harvesting of thermal energy from the self-sustained combustion of cobalt acetate-impregnated flash paper. From left to right: a mini silicon photovoltaic directly converts the intense heat and light into electricity, illuminating the green LED as it approaches the burning surface

4. Conclusions

Flash-paper combustion synthesis provides a rapid, experimentally simple route to producing technologically relevant metals directly from common metal salts. The scope of this work includes the synthesis route for four technological metals (Ag, Cu, Ni, Co), combined with structural, compositional, and functional validation of the resulting materials. Using nitrocellulose sheets as both the combustible matrix and reducing medium, conductive Ag and Cu, as well as magnetic Ni and Co powders, were generated within < 5 s through a self-sustained exothermic reaction under ambient conditions, yielding approximately 5-10 mg per sheet without the need for external chemical reducing agents. XRD and microscopy analyses confirmed the formation of predominantly crystalline metal phases with particle sizes of 30-90 μm and low specific surface areas (< 10 $m^2 \cdot g^{-1}$), while functional tests verified their expected electrical and magnetic behavior. Magnetic measurements confirmed soft ferromagnetic behavior for Ni and Co, while Ag and Cu demonstrated effective electrical conductivity when incorporated into simple circuits.

Compared to sodium borohydride reduction, which is more expensive and yields nanoscale metals where quantum size effects may compromise physical properties, flash-paper combustion synthesis offers a more cost-effective route to bulk-phase metals due to its self-propagating, high-temperature characteristics.

Beyond demonstrating a straightforward synthetic pathway, the results highlight the broader potential of energetic cellulosic substrates as reactive platforms for materials production. The heat released during combustion not only drives chemical transformations but also serves as an energy source that may be exploited for thermal or thermophotovoltaic conversion. This dual functionality-simultaneous materials synthesis and heat generation-positions the method as a promising candidate for energy- and resource-constrained environments.

All in all, the present approach introduces a conceptual framework in which both rapid metal formation and energy capture can be realized at once. Although practical deployment would require careful engineering, controlled atmosphere conditions, and safety considerations, the concept illustrates how combustion-driven processes can couple materials synthesis with energy release. Ongoing work aims to extend flash-paper combustion synthesis beyond the technological metals explored here, toward the generation of precious metals such as gold and platinum.

Availability of data and materials

All data generated or analyzed during this study are included in this article. Also, the related datasets are available from the corresponding author upon reasonable request.

Conflict of interest

The authors have no conflict of interest to disclose.

References

[1] Schlesinger, M. E.; Sole, K. C.; Davenport, W. G.; Alvear Flores, G. R. F. *Extractive Metallurgy of Copper*, 6th ed.; Elsevier: Amsterdam, 2021.

[2] Raabe, D. The materials science behind sustainable metals and alloys. *Chem. Rev.* **2023,** *123*, 2436-2608.

[3] Glavee, G. N.; Klabunde, K. J.; Sorensen, C. M.; Hadjipanayis, G. C. Borohydride reductions of metal ions. A new understanding of the chemistry leading to nanoscale particles of metals, borides, and metal borates. *Langmuir* **1992,** *8*, 771-773.

[4] Cushing, B. L.; Kolesnichenko, V. L.; O'Connor, C. J. Recent advances in the liquid-phase syntheses of inorganic nanoparticles. *Chem. Rev.* **2004,** *104*, 3893-3946.

[5] Bourlinos, A. B.; Polymeros, A.; Papachristodoulou, C.; Moschovas, D.; Avgeropoulos, A.; Salmas, C. E.; Karakassides, M. A. Rapid flash paper combustion synthesis of cobalt blue pigment nanoparticles for use in color 3D printing formulations. *Appl. Funct. Mater.* **2025,** *5*, 19-30.

[6] Bourlinos, A. B.; Moschovas, D.; Avgeropoulos, A.; Maimaris, T. N.; Salmas, C. E.; Karakassides, M. A. Rapid flash-paper combustion synthesis of titania and carbon pigments. *Fine Chem. Eng.* **2026,** *7*, 158-169.

[7] Morris, E.; Pulham, C. R.; Morrison, C. A. Structure and properties of nitrocellulose: Approaching 200 years of research. *RSC Adv.* **2023,** *13*, 32321-32333.

[8] Suwan, T.; Khongkhunthian, S.; Okonogi, S. Silver nanoparticles fabricated by reducing property of cellulose derivatives. *Drug Discov. Ther.* **2019,** *13*, 70-79.

[9] Li, Q.; Yao, G.; Zeng, X.; Jing, Z.; Huo, Z.; Jin, F. Facile and green production of Cu from CuO using cellulose under hydrothermal conditions. *Ind. Eng. Chem. Res.* **2012,** *51*, 3129-3136.

[10] Shankar, R.; Wu, B. B.; Bigioni, T. P. Wet chemical synthesis of monodisperse colloidal silver nanocrystals using digestive ripening. *J. Phys. Chem. C* **2010,** *114*, 15916-15923.

[11] Mott, D.; Galkowski, J.; Wang, L.; Luo, J.; Zhong, C-J. Synthesis of size-controlled and shaped copper nanoparticles. *Langmuir* **2007,** *23*, 5740-5745.

[12] Edinger, S. R.; Gernand, J. M. N_2-BET is a proxy for primary particle size and may not be representative of available specific surface area for aggregated nanoparticle aerosols. *J. Nanosci. Nanotechnol.* **2018,** *18*, 3049-3058.

[13] Shafique, M. K.; Muhmood, T.; Lin, S.; Xiaobin, H.; Gull, S. Synthesis of superfine paramagnetic nickel particles using anionic and cationic surfactants. *Mater. Res. Express* **2019,** *6*, 108001.

[14] Varma, A.; Rogachev, A. S.; Mukasyan, A. S.; Hwang, S. Combustion synthesis of advanced materials: Principles and applications. *Adv. Chem. Eng.* **1998,** *24*, 79-226.

[15] Merzhanov, A. G. The chemistry of self-propagating high-temperature synthesis. *J. Mater. Chem.* **2004,** *14*, 1779-1786.

[16] Rao, R. V. K.; Abhinav, K. V.; Karthik, P. S.; Singh, S. P. Conductive silver inks and their applications in printed and flexible electronics. *RSC Adv.* **2015,** *5*, 77760-77790.

[17] Abhinav, K. V.; Rao, R. V. K.; Karthik, P. S.; Singh, S. P. Copper conductive inks: Synthesis and utilization in flexible electronics. *RSC Adv.* **2015,** *5*, 63985-64030.

[18] Ma, B.; Chaudhary, J. P.; Zhu, J.; Sun, B.; Huang, Y.; Sun, D. Ni nanoparticle-carbonized bacterial cellulose composites for the catalytic reduction of highly toxic aqueous Cr(VI). *J. Mater. Sci.: Mater. Electron.* **2020,** *31*, 7044-7052.

[19] Wang, J.; Liu, M.; Chaemchuen, S.; Klomkliang, N.; Kao, C-M.; Verpoort, F. Carbon-supported cobalt nanoparticles *via* thermal sugar decomposition as efficient electrocatalysts for the oxygen evolution reaction. *ACS Appl. Nano Mater.* **2022,** *5*, 7993-8004.

[20] Fox, P. G.; Ehretsmann, J.; Brown, C. E. The development of internal structure during thermal decomposition: Nickel formate dihydrate. *J. Catal.* **1971,** *20*, 67-73.

[21] Shao, H.; Huang, Y.; Lee, H. S.; Suh, Y. J.; Kim, C. O. Cobalt nanoparticles synthesis from $Co(CH_3COO)_2$ by thermal decomposition. *J. Magn. Magn. Mater.* **2006,** *304*, e28-e30.

[22] Singh, M.; Kumar, M.; Štěpánek, F.; Ulbrich, P.; Svoboda, P.; Santava, E.; Singla, M. L. Liquid-phase synthesis of nickel nanoparticles stabilized by PVP and study of their structural and magnetic properties. *Adv. Mat. Lett.* **2011,** *2*, 409-414.

[23] Yan, H.; Zhang, D.; Xu, J.; Lu, Y.; Liu, Y.; Qiu, K.; Zhang, Y.; Luo, Y. Solution growth of NiO nanosheets supported on Ni foam as high-performance electrodes for supercapacitors. *Nanoscale Res. Lett.* **2014,** *9*, 424.

[24] Khezri, S. H.; Yazdani, A.; Khordad, R.; Ravan, B. A. Preparation of pure cobalt nanoparticles by electric arc discharge method in ethylene glycol. *Mod. Phys. Lett. B* **2013,** *27*, 1350057.

[25] Zhao, X. Q.; Veintemillas-Verdaguer, S.; Bomati-Miguel, O.; Morales, M. P.; Xu, H. B. Thermal history dependence of the crystal structure of Co fine particles. *Phys. Rev. B* **2005,** *71*, 024106.
[26] O'Handley, R. C. *Modern Magnetic Materials: Principles and Applications*, 1st ed.; John Wiley & Sons: New York, 2000.
[27] Gyulasaryan, H.; Manukyan, A.; Bobozhanov, A.; Sheardy, A.; Rogachev, A.; Mukasyan, A. Unique magnetic properties of Ni particles processed by high-energy ball milling. *J. Mater. Res. Technol.* **2025,** *39*, 2387-2395.
[28] Wen, S.; Yao, C.; Wang, D.; Dong, C.; Zhang, X.; May, Y.; Awaji, S.; Watanabe, K. The effect of high magnetic field on electromagnetic response and microwave absorption of cobalt particles during annealing process. *J. Supercond. Nov. Magn.* **2017,** *30*, 463-468.
[29] MEL Science. Exothermic Processes Experiment. https://melscience.com/US-en/articles/exothermic-processes-experiment/ (accessed April 20, 2026).
[30] Coutts, T. J. A review of progress in thermophotovoltaic generation of electricity. *Renew. Sustain. Energy Rev.* **1999,** *3*, 77-184.